

RESEARCH ARTICLE

Knockdown of Mediator Complex Subunit 19 Suppresses the Growth and Invasion of Prostate Cancer Cells

Shengqiang Yu¹*, Yanwei Wang²*, Hejia Yuan¹*, Hongwei Zhao¹, Wei Lv³, Jian Chen², Fengchun Wan¹, Dongfu Liu¹, Zhenli Gao¹, Jitao Wu¹*

1 Department of Urology, the Affiliated Yantai Yuhuangding Hospital of Qingdao University, Yantai, Shandong, China, **2** Central Laboratory, the Affiliated Yantai Yuhuangding Hospital of Qingdao University, Yantai, Shandong, China, **3** Department of Nephrology, the Affiliated Yantai Yuhuangding Hospital of Qingdao University, Yantai, Shandong, China

* These authors contributed equally to this work.

* agourodman@163.com (SY); jtwu1006@163.com (JW)



OPEN ACCESS

Citation: Yu S, Wang Y, Yuan H, Zhao H, Lv W, Chen J, et al. (2017) Knockdown of Mediator Complex Subunit 19 Suppresses the Growth and Invasion of Prostate Cancer Cells. *PLoS ONE* 12(1): e0171134. doi:10.1371/journal.pone.0171134

Editor: Aamir Ahmad, University of South Alabama Mitchell Cancer Institute, UNITED STATES

Received: October 9, 2016

Accepted: January 16, 2017

Published: January 26, 2017

Copyright: © 2017 Yu et al. This is an open access article distributed under the terms of the [Creative Commons Attribution License](https://creativecommons.org/licenses/by/4.0/), which permits unrestricted use, distribution, and reproduction in any medium, provided the original author and source are credited.

Data Availability Statement: All relevant data are within the paper and its Supporting Information files.

Funding: This study was supported by National Natural Science Foundation of China (81302234, <http://www.nsf.gov.cn/>); National Natural Science Foundation of China (81572835, <http://www.nsf.gov.cn/>); and Shandong Provincial Natural Science Foundation (ZR2013HL070, <http://www.sdnsf.gov.cn/portal/>).

Competing Interests: The authors have declared that no competing interests exist.

Abstract

Prostate cancer (PCa) is one of the most common cancers in elderly men. Mediator Complex Subunit 19 (Med19) is overexpressed and plays promotional roles in many cancers. However, the roles of Med19 in PCa are still obscure. In this study, by using immunohistochemical staining, we found higher expression level of Med19 in PCa tissues than in adjacent benign prostate tissues. We then knocked down the Med19 expression in PCa cell lines LNCaP and PC3 by using lentivirus siRNA. Cell proliferation, anchor-independent growth, migration, and invasion were suppressed in Med19 knockdown PCa cells. In nude mice xenograft model, we found that Med19 knockdown PCa cells formed smaller tumors with lower proliferation index than did control cells. In the mechanism study, we found that Med19 could regulate genes involved in cell proliferation, cell cycle, and epithelial-mesenchymal transition, including P27, pAKT, pPI3K, IGF1R, E-Cadherin, N-Cadherin, Vimentin, ZEB2, Snail-1 and Snail-2. Targeting Med19 in PCa cells could inhibit the PCa growth and metastasis, and might be a therapeutic option for PCa in the future.

Introduction

Prostate cancer (PCa) is one of the most common cancers in western world, with a leading cause of mortality and morbidity [1]. Early detection and treatment have improved the survival rate significantly. However, 20~40% of patients undergoing radical prostatectomy and 30~50% of patients undergoing radiotherapy will have biochemical recurrence within 10 years [2]. For advanced PCa, androgen deprivation therapy (ADT) is still the first therapeutic option [3]. Although initially effective at blocking tumor progression, ADT eventually fails by leading PCa to a castration-resistant stage. Many efforts have been made to seek more effective therapeutic methods for PCa [4].

Mediator complex subunit 19 (Med19) binds to gene-specific regulatory factors and provides support for the basal RNA polymerase II transcription machinery. Med19 has been

implicated in the progress of several cancers, and knockdown of its expression may inhibit the progression of these cancers [5–8]. However, the roles of Med19 on PCa growth and invasion are still obscure.

In the present study, we performed immunohistochemical (IHC) staining to compare the Med19 expression levels in human PCa tissues and adjacent benign prostate tissues. Then we knocked down the Med19 expression in PCa cell lines LNCaP and PC3 by using lentivirus siRNA to study the *in vitro* proliferation, cell cycle, anchor-independent growth, migration, and invasion of PCa cells. For the *in vivo* study, we inoculated the resultant PC3 cells subcutaneously to athymic nude mice to determine the tumor growth. For the mechanism, we performed quantitative reverse transcription polymerase chain reaction (Q-PCR) and Western blot assays to detect multiple genes relevant to proliferation, cell cycle, and metastasis.

Materials and Methods

IHC Staining

We collected 10 pairs of paraffin-embedded human PCa tissues and adjacent non-cancerous tissues (from 01-February-2014 to 30-August-2015) from Paraffin-embedded Tissue Bank of the Affiliated Yantai Yuhuangding Hospital of Qingdao University. The use of human tissues was approved by the Ethics Committee of the Affiliated Yantai Yuhuangding Hospital of Qingdao University. For IHC staining, after routine rehydration, antigen retrieval, and blocking, the sections were incubated in the primary antibody at 4°C overnight. The primary anti-Med19 antibody (1:200, Rabbit Polyclonal, HPA039912 Sigma-Aldrich) was recognized by the biotinylated secondary antibody and visualized by Vectastain avidin-biotin complex peroxidase system (ABC kit, VECTOR Laboratories) and peroxidase substrate 3,3'-diaminobenzidine kit (DAB kit, VECTOR Laboratories).

Cell Culture and Lentivirus Infection

The human PCa cell lines LNCaP and PC3 were kind gifts from Dr. Shujie Xia of Shanghai Jiaotong University. All cells were cultured in RPMI 1640 supplemented with 10% fetal bovine serum (FBS), 100 units/ml penicillin, and 100 µg/mL streptomycin at 37°C in a humidified incubator containing 5% CO₂.

To knock down the Med19 in LNCaP and PC3 cells, we performed the lentivirus infection strategy. Lentivirus containing siRNA targeting Med19 gene (5' -GTAGCTCTTTCAATCCTAT-3') or nonsilencing control (5' -TTCTCCGAACGTGTCACGT-3') were constructed by GeneChem, Shanghai, China. The day before infection, cells were plated at a density of 20~30% in a good condition. The above lentivirus (containing fluorescence) was treated to the LNCaP and PC3 cells according to the manufacture's protocol. The culture medium was changed to normal medium 10 hours after infection. Three days later, the cells were subjected to fluorescence activated cell sorting (FACS) with flow cytometer for further experiments.

Q-PCR

Total RNA was extracted and purified using Trizol (Takara, Carlsbad, CA). Three µg RNA was subjected to reverse transcription using Superscript III (TransGene, Beijing, China). Amplification was performed using SYBR green as fluorescent with the following PCR amplification conditions: 1 cycle at 95°C for 10 min, 45 cycles at 95°C for 15 sec and 60°C for 60 sec [9]. The relative expression of mRNA was calculated using the $2^{-\Delta\Delta CT}$ to compare the expression levels among different samples. The primer sequences were as follows (5'-3'): Med19: Forward "TGC CAGGGATGATTGATCTG", Reverse "TCTTCTTGGGAGGCTGAATATG"; IGF1R: Forward "CTG

GCTCCGGAGGAGGGTCC”, Reverse “AATACATCTCCAGCCTCCTTAG”; N-Cadherin: Forward “TCAGGCGTCTGTAGAGGCTT”, Reverse “ATGCACATCCTTCGATAAGACTG”; E-cadherin: Forward “CTCCCAATACATCTCCCTTAC”, Reverse “AGGTGGTCACTTGGTCTTTATT”; Vimentin: Forward “AGTCCACTGAGTACCGGAGAC”, Reverse “CATTTACGCATCTGGC GTTC”; ZEB-2: Forward “CAAGAGGCGCAAACAAGCC”, Reverse “GGTTGGCAATACCGT CATCC”; Snail-1: Forward “TCGGAAGCCTAACTACAGCGA”, Reverse “AGATGAGCATTGG CAGCGAG”; Snail-2: Forward “CGAACTGGACACACATACAGTG”, Reverse “CTGAGGATCTCT GGTGTGGT”; β -actin: Forward “GGCGGCACCACCATGTACCCT”, Reverse “AGGGGCCGGAC TCGTCATACT”.

Western Blot Analysis

The LNCaP-Med19-si/sc and PC3-Med19-si/sc cells were cultured in 10% FBS to 90% confluence, then were lysed in RIPA lysis buffer, separated on 8% SDS PAGE gel, and transferred to polyvinylidene difluoride (PVDF) membrane [9]. After blocked by 5% nonfat milk in PBST buffer, the membrane was incubated in the primary antibody and then in HRP-conjugated secondary antibodies. The primary antibodies used were: anti-Med19 (1:400, Rabbit Polyclonal, HPA039912 Sigma-Aldrich), anti-P27 (1:800, Rabbit Polyclonal, #2252 Cell Signaling Technology), anti-pAKT (1:1000, Rabbit Polyclonal, #9271 Cell Signaling Technology), anti-pPI3K (1:200, Rabbit Polyclonal, sc-293115 Santa Cruz Biotechnology), anti-GAPDH (1:500, Mouse monoclonal, sc-47724 Santa Cruz Biotechnology). Immunoreactive bands were detected by the chemiluminescent detection system (ECL, Pierce, Rockford, IL, USA)

Methyl Thiazolyl Tetrazolium (MTT) Assay

The LNCaP-Med19-si/sc and PC3-Med19-si/sc cells were seeded in 24-well plates (1×10^4 cells per well) and incubated with RPMI 1640 with 10% FBS in 37°C and 5% CO₂ incubator with medium changed every 48 hours. The plates were stained with MTT (Sigma) at day 0, 2, 4, and 6 for 3 hours. The absorbency was read at a test wave length of 570 nm.

Cell Cycle Analysis

Cells were fixed in 70% ice-cold ethanol and stained with propidium iodide (PI) (40 μ g/ml) in RNase (100 μ g/ml). Cells were analyzed using a FACScan flow cytometer (Becton Dickinson, San Jose, CA) and all groups were performed in triplet and statistically analyzed.

Soft Agar Assay (Anchor-independent Colony Formation Assay)

Each well of the six-well plate was laid with a base layer of 0.5 mL of 1% DNA grade agarose. The 1% melted DNA grade agar (at 40°C), 3 \times RPMI 1640 medium, and cell suspension were mixed by a ratio of 1:1:1, and come to a final cell concentration of 10^4 cells/ml for PC3-Med19-si/sc cells and 5×10^4 cells/ml for LNCaP-Med19-si/sc cells. One ml of the mixture was added on the top of the base agar. After coagulation, 2 ml RPMI 1640 supplemented with 10% FBS was added, and medium was replaced every 3 days to supply the nutrition. After 2 weeks' culture in 37°C incubator, the colonies were stained by 1mg/ml INT (Sigma) solution.

Invasion Assay

LNCaP-Med19-si/sc (1×10^5) or PC3-Med19-si/sc (5×10^4) cells in serum free RPMI 1640 medium was added to the cell culture inserts with microporous (8 μ m) membrane with or without Matrigel coating (control insert). RPMI 1640 medium containing 10% FBS was added to the bottom chamber. The cells were then incubated for 22 hours at 37°C, and the upper

chamber was removed. The cells on the bottom of the upper chambers were stained with 1% toluidine blue, and the number of cells was counted under a microscope. The invasion ratio was the ratio of the number of cells invading through Matrigel coated insert membrane against the number of those migrated through non-coated insert membrane.

Wound Healing Assay

The LNCaP-Med19-si/sc and PC3-Med19-si/sc cells were seeded in a 6-cm dish and cultured to confluency. The cell monolayer was scraped firmly with a plastic pipette tip and then left growing at 37°C. The "wounded" areas were photographed by a phase contrast microscopy in 0 and 24 hours after scraping. The percentage of wound healing area was calculated.

Xenograft Model of Tumor Growth *in vivo*

Male immune-deficient BALB/c nude mice (4–6 weeks old) were purchased from Beijing Weitong Li-hua Laboratory Animals and Technology Ltd. The cells (1×10^6) were suspended in 50 μ l Matrigel (BD Biosciences, Franklin Lakes, NJ, USA) and then implanted subcutaneously into the left flank (PC3-Med19-sc) and right flank (PC3-Med19-si) of nude mice. The inoculation sites were checked twice a week until tumors were palpable. Then the tumors were measured 3 times a week. All mice were observed daily for food, water, bedding, and general health conditions. The criteria of humane endpoints were as follows: Body Condition Score < 2; any single tumor > 2000 mm³, or multiple tumors > 3000 mm³, or any tumor interferes with basic bodily functions; the tumor becomes ulcerated or necrotic; the animal's ability to eat, drink, or breath is significantly impaired. All 6 mice survived well at 6 weeks after inoculation and were sacrificed by CO₂. The tumors were harvested and weighed to compare between groups. The care and use of nude mice in this study were approved by the Ethics Committee of the Affiliated Yantai Yuhuangding Hospital of Qingdao University. All procedures abide by the 1964 Helsinki declaration and its later amendments or comparable ethical standards.

Apoptosis Assay

Apoptotic cells were detected by terminal deoxynucleotidyl transferase-mediated biotinylated deoxyuridine triphosphate nick end labeling (TUNEL) assay as recommended by the manufacturer (Roche). Briefly, paraffin-embedded tissue was deparaffinized, digested with proteinase K (20 μ g/ml) for 15 minutes at room temperature, then was labeled for 60 minutes at room temperature and mounted (with DAPI).

Statistical Analysis

Numerical data were presented as mean \pm standard deviation. Statistical analysis between groups was performed by using two-sided Student's T test. *P* values < 0.05 were considered statistically significant.

Results

Med19 Expression Level Was Elevated in PCa Tissues

We performed IHC staining to test the Med19 expression in 10 pairs of PCa tissues and adjacent benign tissues, and found that Med19 expression level was much higher in PCa tissues (Fig 1A and 1B) than in adjacent benign tissues (Fig 1C and 1D), which indicated that Med19 was up-regulated in PCa tissues. This data encouraged us to continue studying the Med19 roles by using the PCa cell lines LNCaP and PC3.

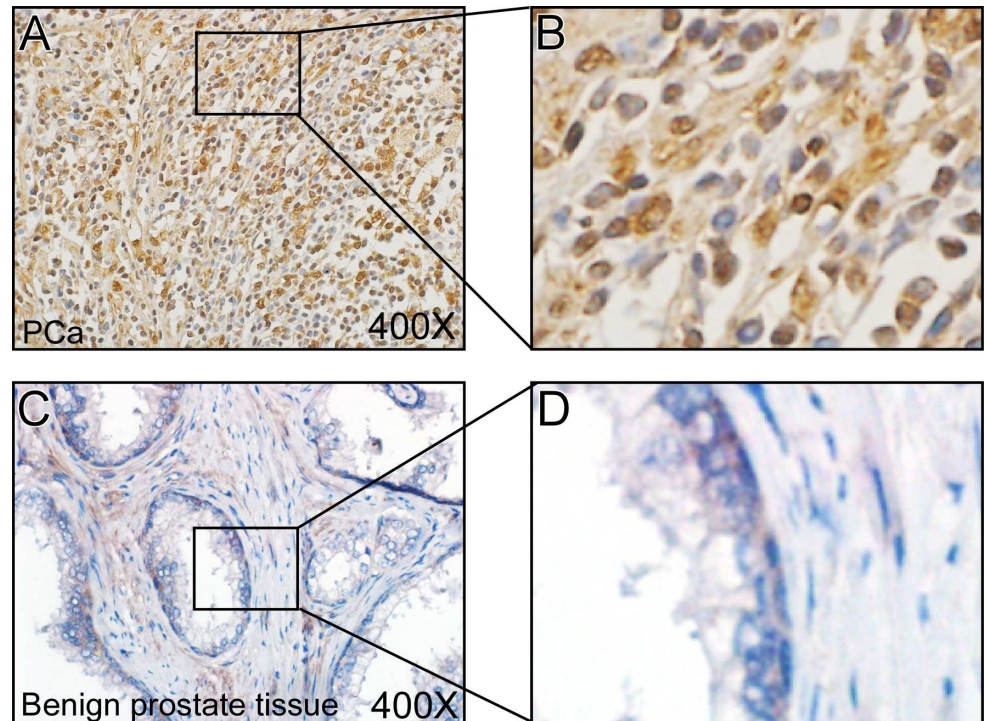


Fig 1. Med19 expression level was elevated in PCa tissues. Med19 IHC staining was performed in 10 pairs of PCa and adjacent benign prostate tissues. The Med19 expression level was much higher in PCa tissues (A, B) than in adjacent benign tissues (C, D). (A) and (C) were taken at 400×magnification, (B) and (D) were local amplified pictures.

doi:10.1371/journal.pone.0171134.g001

Knockdown of Med19 with Lentiviral Infection in PCa Cells

Since Med19 expresses at high levels in both LNCaP and PC3 cells, we performed lentivirus siRNA knockdown strategy. The LNCaP and PC3 cells were infected with lentivirus that contained either siMed19 or control scramble RNA, then were sorted by FACS to establish relatively stable cells of LNCaP-Med19-si and PC3-Med19-si, as well as their control cells of LNCaP-Med19-sc and PC3-Med19-sc. Efficient transduction was confirmed by determining the GFP expression in a fluorescent microscope (Fig 2A). The GFP positive rate was more than 95% in both cell lines. In mRNA level, the relative Med19 expression was $26.18 \pm 5.27\%$ in LNCaP-Med19-si cells, and $16.88 \pm 3.40\%$ in PC3-Med19-si cells (Fig 2B). We further determined the Med19 expression level with Western blot. Compared to the control cells, the Med19 protein expression level was dramatically decreased in LNCaP-Med19-si and PC3-Med19-si cells (Fig 2C).

Knockdown of Med19 Inhibited PCa Cells Growth via Cell Cycle Arrestment

In MTT assay, the LNCaP-Med19-si and PC3-Med19-si cells grew much slower than their control cells (Fig 3A). MTT assay could only reflect the cell growth ability in attached conditions. For tumor cells, the anchor-independent growth is an important property for their malignancy. The soft agar assay was performed to evaluate the anchor-independent growth of the PCa cells. After 2 weeks culture in soft agar, the LNCaP-Med19-si and PC3-Med19-si cells formed much less colonies than control cells (Fig 3B). To determine whether down-regulation

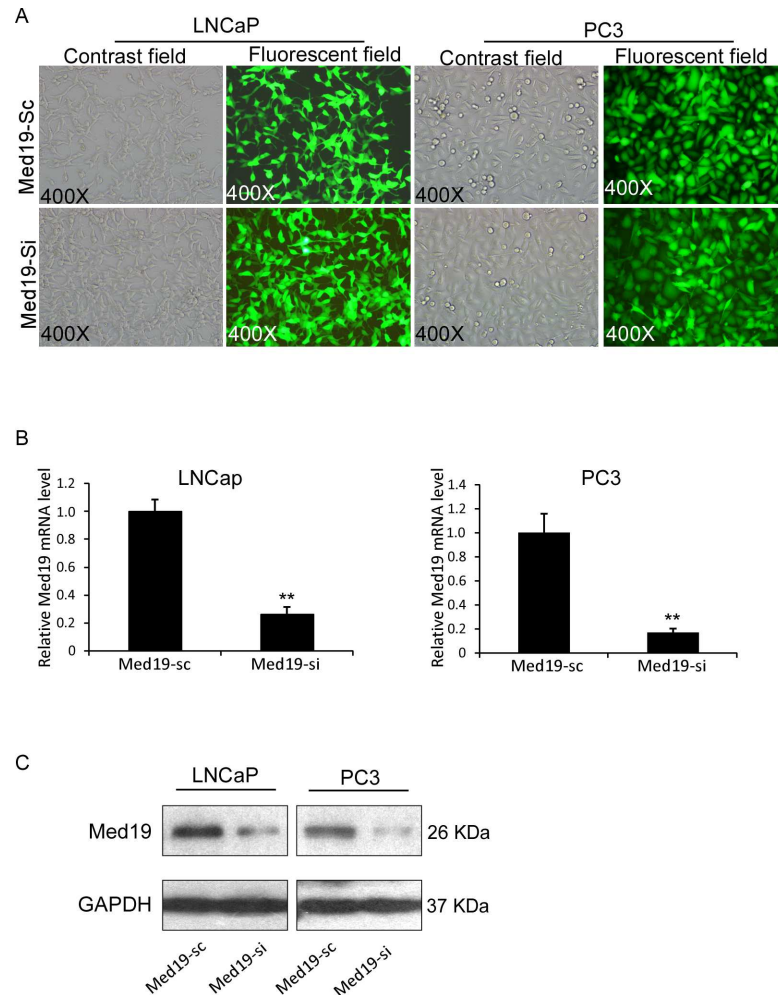


Fig 2. Establishment and characterization of LNCaP-Med19-si/sc and PC3-Med19-si/sc cells. (A) After lentivirus infection and FACS sorting, the transduction efficiency was confirmed by determining the GFP expression in a fluorescent microscope. The GFP positive rate was more than 95% in all cells. (B) In Q-PCR assay, the relative Med19 expression levels were 26.18±5.27% in LNCaP-Med19-si cells (n = 3, **P<0.01), and 16.88±3.40% in PC3-Med19-si cells (n = 3, **P<0.01). (C) In Western blot assay, the Med19 expression level was dramatically decreased in LNCaP-Med19-si and PC3-Med19-si cells. GAPDH was used as an internal control.

doi:10.1371/journal.pone.0171134.g002

of Med19 could impact the cell cycle of PCa cells, the flow cytometry cell cycle analysis was performed. Compared with control cells, the proportion of G0/G1 phase cells was significantly increased in the LNCaP-Med19-si and PC3-Med19-si cells (Fig 3C), which indicated that knockdown of Med19 resulted in cell cycle arrest in G0/G1 phase.

Knockdown of Med19 Inhibited PCa Cell Invasion and Migration *in vitro*

Invasion and migration abilities are important for the metastasis of tumor cells. An intro chamber invasion assay was performed to detect the invasion ability of PCa cells. After 22 hours' culture in the Boyden chambers, much fewer LNCaP-Med19-si cells (invasion ratio of 4.26±0.92% v.s.11.74±1.94% P<0.01) and PC3-Med19-si cells (invasion ratio of 19.71±4.00% v.s.32.27±3.72%, P<0.05) invaded through the Matrigel membrane than their control cells (Fig 4A). To test the migration ability, a wound healing assay was performed. The PCa cells in

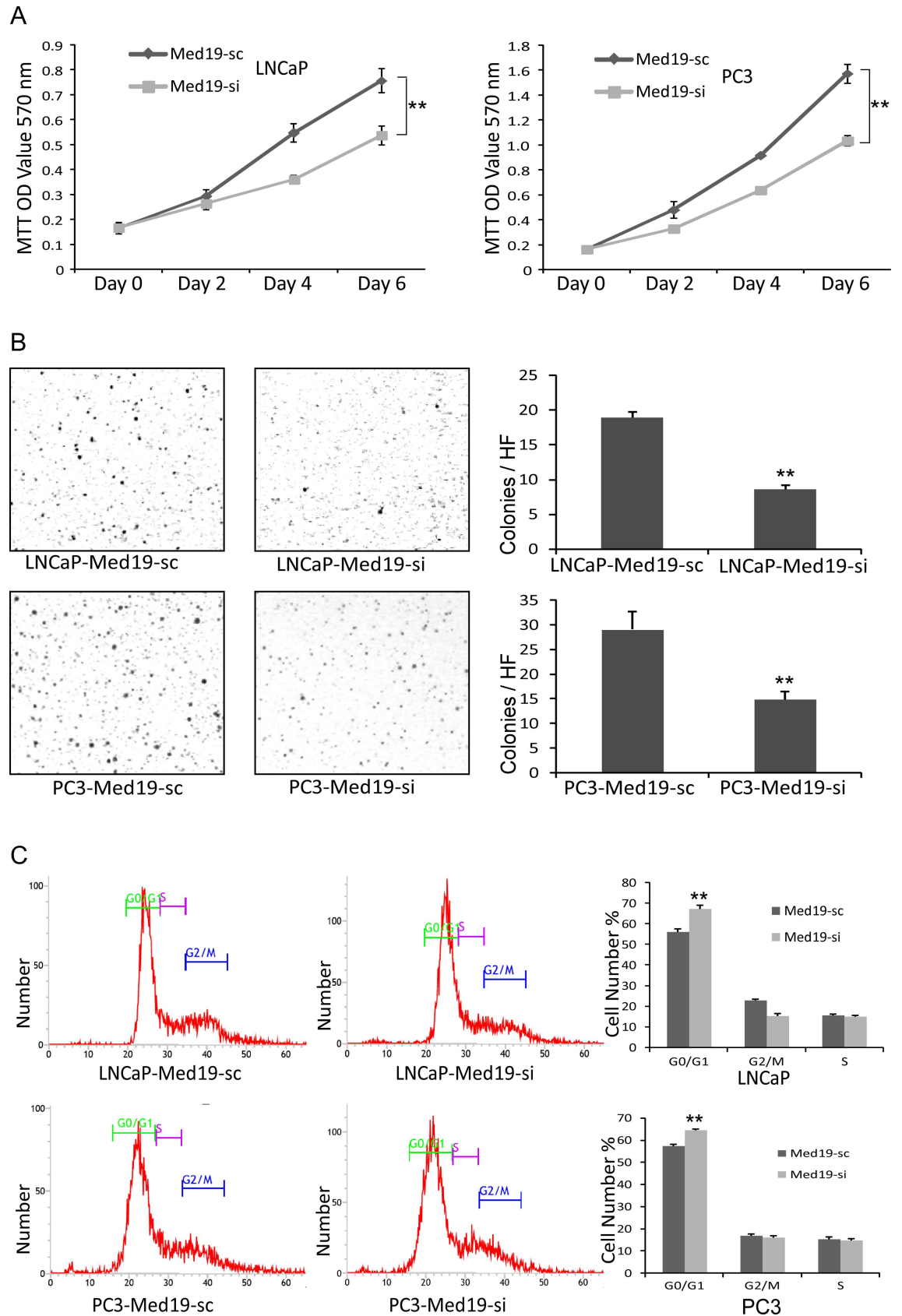


Fig 3. Knockdown of Med19 inhibited cell growth via arresting cell cycle. (A) In MTT assay, the growth curves showed the LNCaP-Med19-si and PC3-Med19-si cells grew much slower than the control cells. ($n = 3$, $**P < 0.01$). (B) In colony formation assay (soft agar assay), the LNCaP-Med19-si cells formed 8.61 ± 0.51 colonies/HF, and the LNCaP-Med19-sc cells formed 18.89 ± 0.82 colonies/HF. ($n = 3$, $**P < 0.01$). The PC3-Med19-si cells formed 14.89 ± 1.51 colonies/HF, and the PC3-Med19-sc cells formed 29.06 ± 3.62 colonies/HF. ($n = 3$, $**P < 0.01$). (C) In flow cytometry cell cycle analysis, the proportion of G0/G1 phase cells was significantly increased in LNCaP-Med19-si and PC3-Med19-si cells. The proportion of G0/G1 was $67.29 \pm 1.70\%$ in LNCaP-Med19-si cells and $56.23 \pm 1.46\%$ in LNCaP-Med19-sc cells ($n = 3$, $**P < 0.01$). The proportion of G0/G1 was $64.39 \pm 0.62\%$ in PC3-Med19-si cells and $57.29 \pm 0.97\%$ in PC3-Med19-sc cells ($n = 3$, $**P < 0.01$).

doi:10.1371/journal.pone.0171134.g003

culture dishes were scraped with a plastic pipette tip to generate the same size of “wound” area, then continue to culture for 24 hours. Compared to control cells, the wound healing areas were much smaller in the LNCaP-Med19-si cells ($8.83 \pm 2.56\%$ v.s. $15.83 \pm 4.62\%$, $P < 0.01$) and PC3-Med19-si cells ($70.83 \pm 9.37\%$ v.s. $87.33 \pm 4.63\%$, $P < 0.01$) (Fig 4B).

Knockdown of Med19 Inhibited PCa Progression *in vivo*

To confirm the Med19 roles in PCa tumor growth *in vivo*, a xenograft tumor model was established in nude mice. The PCa cells were inoculated subcutaneously into nude mice flank areas. Since the LNCaP cells were difficult to form tumor in nude mice, we only collected the data of PC3 cells. Six weeks after cells inoculation, the tumors were harvested and weighed. The PC3-Med19-si cells formed much smaller tumors than their control tumors (0.17 ± 0.08 g v. 0.38 ± 0.19 g, $P < 0.05$) (Fig 5A). To test the proliferation rate of the xenograft tumors, Ki67 IHC staining was performed. There were fewer Ki67 positive cells in PC3-Med19-si tumors than control tumors. The proliferation index was $18.30 \pm 6.55\%$ in PC3-Med19-si tumors, but $33.22 \pm 4.36\%$ in control tumors, $P < 0.05$ (Fig 5B). The TUNEL assay was used to further determine the apoptotic cells in the xenograft tumors. However, the ratio of apoptotic cells did not come to a statistical significance between groups (Fig 5C).

Knockdown of Med19 Altered the Cell Growth, Cell Cycle, and Epithelial–Mesenchymal Transition (EMT) Related Genes

In Western blot assay, the pAKT and pPI3K expression levels decreased, and P27 expression level increased in the Med19 knockdown cells (Fig 6A). In Q-PCR analysis, the IGF1R expression was down-regulated (Fig 6B and 6C), and many EMT related genes including E-Cadherin, N-Cadherin, Vimentin, ZEB2, Snail-1, and Snail-2 were altered in the Med19 knockdown cells (Fig 6B and 6C).

Discussion

Med19 is a component of the Mediator complex, which involved in the transcription regulation of nearly all RNA polymerase II-dependent genes [10]. Med19 is important in stabilizing the entire Mediator complex, making it critical to the transcriptional regulation [11]. Absence of Med19 may decrease the binding affinity of Mediator with RNA Polymerase II [11].

Med19 has been reported in the progress of several cancers, and knockdown of its expression may inhibit the growth and spread of these cancers. In bladder urothelial carcinoma, the Med19 was reported to promote cancer cell growth, bone metastasis, and invasiveness by regulating cell cycles and bone morphogenetic protein 2 [8, 12]. In breast cancer, Med19 may promote cell proliferation by regulating CBFA2T3/HEB expression [13]. In lung cancer, MED19 could promote tumor proliferation, tumorigenesis, metastasis, and enhance chemo-sensitivity to cisplatin in non-small cell lung cancer cells [14–16]. The Med19 has been reported to promote tumor growth and/or metastasis in ovarian cancer, gastric cancer, pancreatic cancer, osteosarcoma, and liver cancer [5–7, 17–18]. However, there are few reports about the roles of

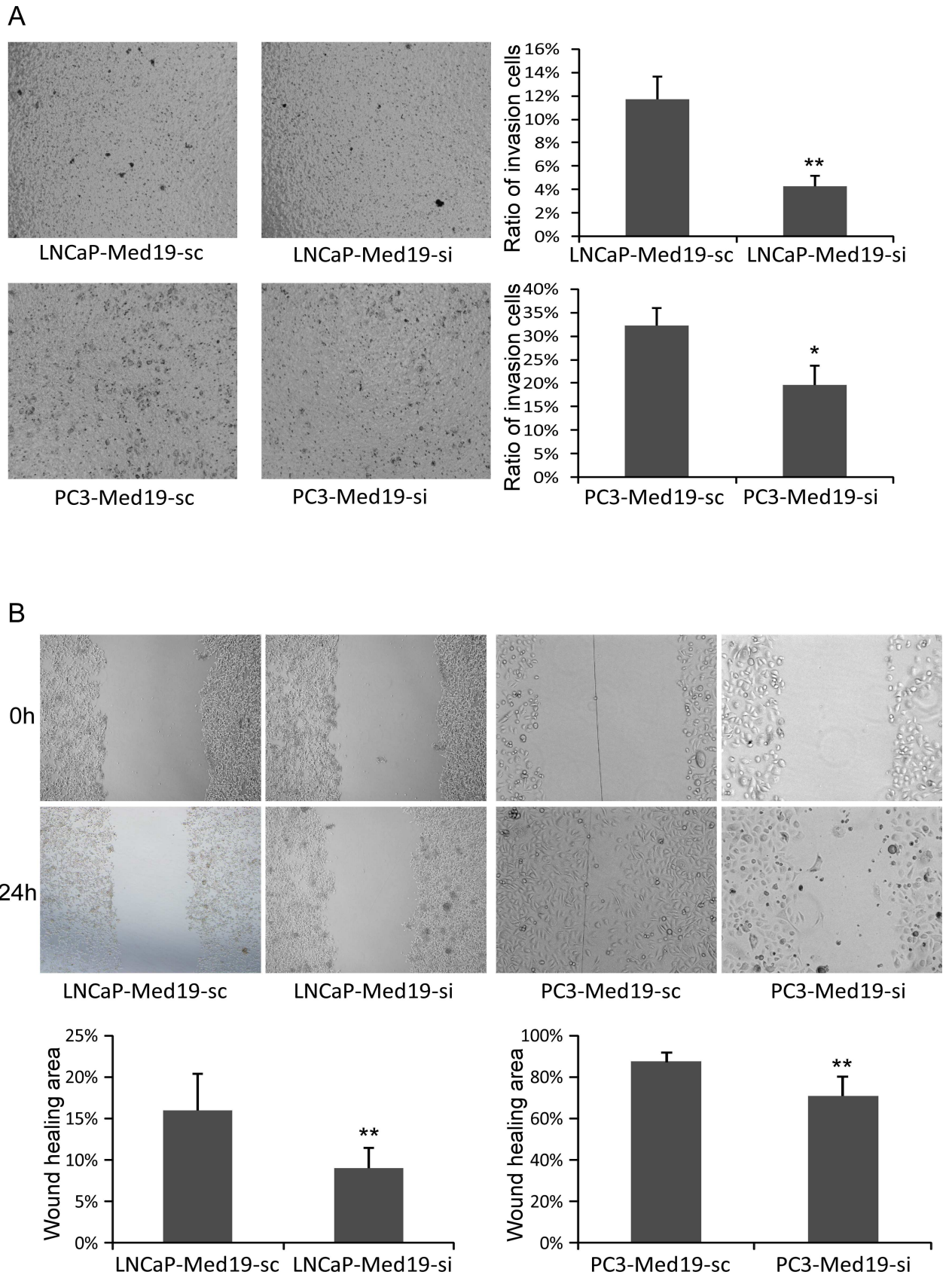


Fig 4. Knockdown of Med19 inhibited PCa cells invasion and migration *in vitro*. (A) In invasion assay, the invasion ratio was $4.26 \pm 0.92\%$ in LNCaP-Med19-si cells and $11.74 \pm 1.94\%$ in LNCaP-Med19-sc cells ($n = 3$, $**P < 0.01$). The invasion ratio was $19.71 \pm 4.00\%$ in PC3-Med19-si cells and $32.27 \pm 3.72\%$ in PC3-Med19-sc cells ($n = 3$, $*P < 0.05$). (B) In “wound healing” migration assay, after 24 hours culture, the percentage of wound healing area was $8.83 \pm 2.56\%$ in LNCaP-Med19-si cells and $15.83 \pm 4.62\%$ in LNCaP-Med19-sc cells ($n = 3$, $**P < 0.01$), $70.83 \pm 9.37\%$ in PC3-Med19-si cells and $87.33 \pm 4.63\%$ in PC3-Med19-sc cells ($n = 3$, $**P < 0.01$).

doi:10.1371/journal.pone.0171134.g004

Med19 in PCa. Cui et al [19] reported Med19 could promote the proliferation and tumorigenesis and induce apoptosis in human prostate cancer cells. Imberg-Kazdan et al [20] found that

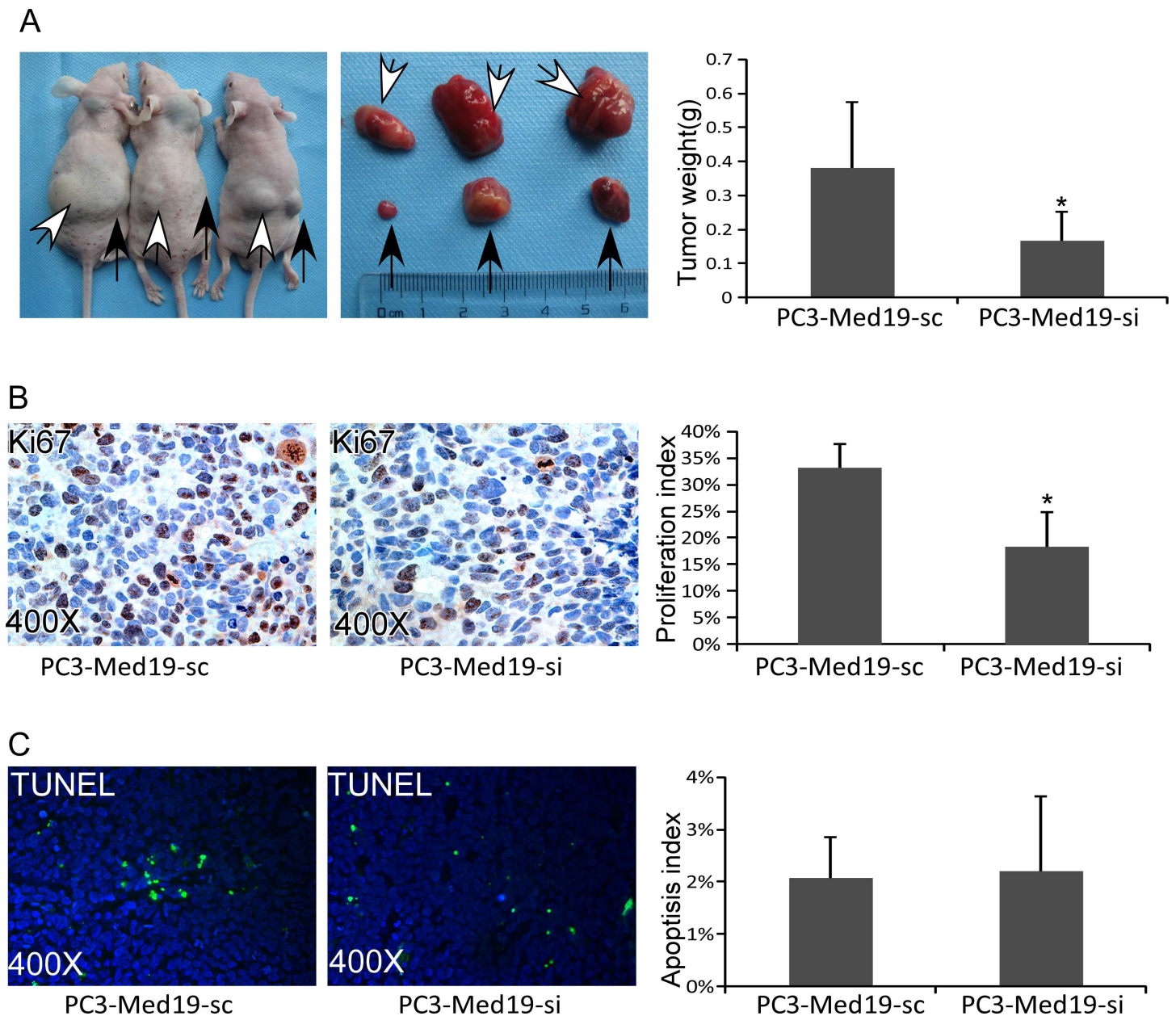


Fig 5. Knockdown of Med19 inhibited PCa progression in nude mice. (A) Six weeks after inoculation, PC3-Med19-si (black arrows showed tumors in the right flank) and PC3-Med19-sc (white arrows showed tumors in the left flank) formed tumors in nude mice. The weight of PC3-Med19-si and PC3-Med19-sc tumors was $0.17 \pm 0.08\text{g}$ v.s. $0.38 \pm 0.19\text{g}$ ($n = 6$, $*P < 0.05$). (B) In Ki67 IHC staining, the PC3-Med19-si tumors had fewer positive cells than PC3-Med19-sc tumors. The proliferation index was $18.30 \pm 6.55\%$ in PC3-Med19-si tumors and $33.22 \pm 4.36\%$ in control tumors ($n = 6$, $*P < 0.05$). (C) In TUNEL assay, the apoptotic cells were similar in both tumors. The apoptosis index in PC3-Med19-si and PC3-Med19-sc tumors was $2.21 \pm 1.43\%$ v.s. $2.08 \pm 0.78\%$ ($n = 6$, $P > 0.1$).

doi:10.1371/journal.pone.0171134.g005

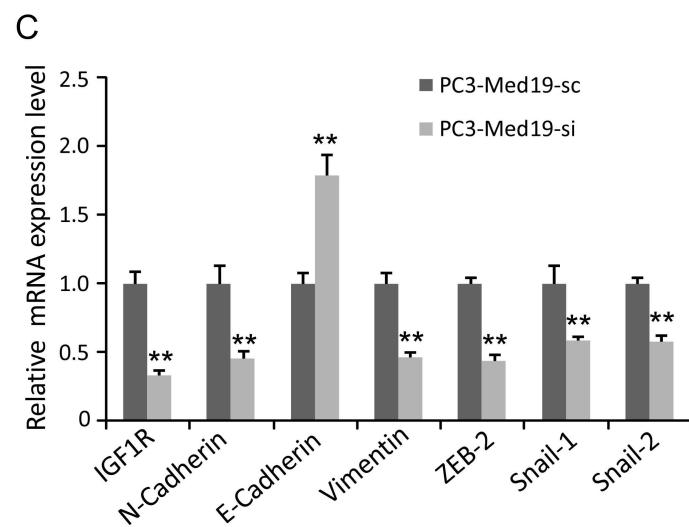
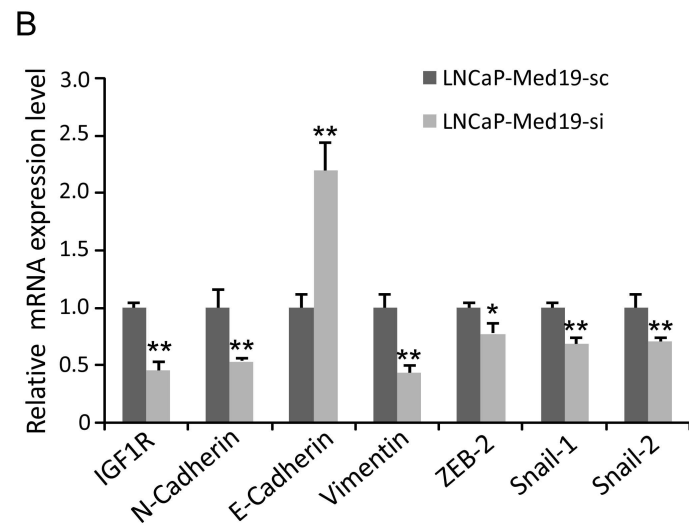
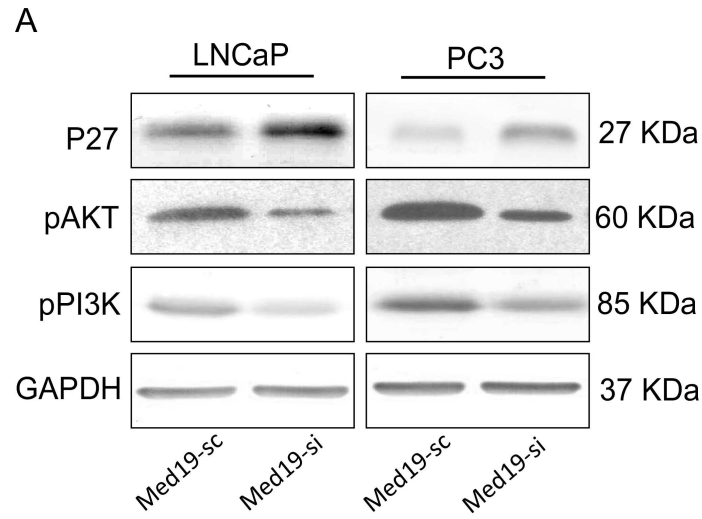


Fig 6. Knockdown of Med19 altered multiple genes expression in PCa cells. (A) In Western blot assay, the pAKT and pPI3K expression levels were lower, and the P27 expression level was higher in the Med19 knockdown cells. GAPDH was used as an internal control. (B, C) In Q-PCR assay, the IGF1R, N-Cadherin, Vimentin, ZEB2, Snail-1, and Snail-2 were down-regulated, and the E-Cadherin was up-regulated in both LNCaP-Med19-si and PC3-Med19-si cells (n = 3, *P<0.05, **P<0.01).

doi:10.1371/journal.pone.0171134.g006

depletion of HIPK2 and MED19 in human prostate cancer cells decreased AR target gene expression and reduced the proliferation of androgen-dependent and castration-resistant prostate cancer cells.

In the present study, we performed Me19 IHC staining on human PCa tissues and adjacent benign prostate tissues, and found Med19 expression level was elevated in PCa tissues. We then knocked down the Med19 expression in PCa cell lines LNCaP and PC3 by using lentivirus siRNA. The cell proliferation, anchor-independent growth, migration, invasion abilities were suppressed in Med19 knockdown PCa cells. More Med19 knockdown PCa cells were arrested in G0/G1 phase. By using nude mice xenograft PCa model, we found the Med19 knockdown PCa cells formed smaller tumors and had lower proliferation index. For the mechanism, we found Med19 could regulate the expression of multiple genes relevant to tumor growth and metastasis, including P27, pAKT, pPI3K, IGF1R, E-Cadherin, N-Cadherin, Vimentin, ZEB2, Snail-1 and Snail-2.

PI3K/AKT is important in regulating the cell cycle [21]. PI3K activation phosphorylates and activates AKT, and AKT has a number of downstream effects including inhibition of p27 [22]. P27, also known as Kip1, is a cyclin-dependent kinase inhibitor [23]. It is well known that P27 could suppress tumor cells proliferation by regulating the cell cycle [24]. IGF1R, belonging to the large class of tyrosine kinase receptors, plays promotional roles in PCa progression [25]. Our data suggested that the Me19 could promote PCa tumor growth by regulating pAKT, pPI3K, P27, and IGF1R expression level.

In the EMT process, epithelial cells lose their polarity and gain migratory and invasive properties. Initiation of cancer metastasis requires invasion, which is enabled by EMT [26]. In our study, the EMT related genes N-Cadherin, Vimentin, ZEB2, Snail-1 and Snail-2 expression levels decreased and E-Cadherin expression level increased in Med19 knockdown cells. This suggested that Me19 could increase PCa tumor metastatic abilities by promoting EMT.

Overall, in the present study, we found that Med19 could promote PCa growth and metastasis by regulating the cell proliferation, cell cycle, and EMT-related genes. Targeting the Med19 in PCa cells could inhibit the PCa growth and metastasis, and might be a therapeutic option for PCa in the future.

Supporting Information

S1 Fig. The volume of subcutaneous tumors in nude mice. Six weeks after inoculation, PC3-Med19-si and PC3-Med19-sc formed tumors in nude mice. The PC3-Med19-si tumor volume was $211.8 \pm 123.7 \text{ mm}^3$, and the PC3-Med19-sc tumor volume was $462.2 \pm 233.3 \text{ mm}^3$ (n = 6, *P<0.05). The tumor volume was calculated by the formula “Volume = $\pi/6$ (L×W×H)”. (TIF)

S2 Fig. The expression of apoptosis related genes was not altered in Med19 knockdown cells. In Q-PCR assay, the Bax, Bcl-2, Caspase-3, and Caspase-8 expression levels were not altered in LNCaP-Med19-si and PC3-Med19-si cells (n = 3, *P<0.05). The primer sequences are as follows: Bax: Forward “TCATGGGCTGGACATTGGAC”, Reverse “GAGACAGGGACATCAGTCGC”; Bcl-2: Forward “TGGATGACTGAGTACCTGAACC”, Reverse “CGCATCTCGGACC TGTGG”; Caspase-3: Forward “GCGGTTGTAGAAGTTAATAAAGGT”, Reverse “ATTCGCTTC

CATGTATGATCTTTGG”; Caspase-8: Forward “GGAACCTTCAGACACCAGGCA”, Reverse “CCTC CGCCAGAAAGGTACAG”.
(TIF)

Acknowledgments

Thanks Dr. Jiahui Wang (from Central Laboratory, the Affiliated Yantai Yuhuangding Hospital of Qingdao University) for the English proofreading.

Author Contributions

Conceptualization: SY YW HY JW.

Formal analysis: JC FW.

Funding acquisition: SY JW HZ.

Investigation: SY YW HY DL.

Methodology: HZ WL.

Project administration: ZG JW.

Resources: JC ZG.

Supervision: ZG JW.

Validation: HZ WL JC FW.

Writing – original draft: SY YW HY.

Writing – review & editing: JW ZG JC.

References

1. Wong MC, Goggins WB, Wang HH, Fung FD, Leung C, Wong SY, et al. Global Incidence and Mortality for Prostate Cancer: Analysis of Temporal Patterns and Trends in 36 Countries. *Eur Urol*. 2016. Epub 2016/06/13.
2. Paller CJ, Antonarakis ES. Management of biochemically recurrent prostate cancer after local therapy: evolving standards of care and new directions. *Clin Adv Hematol Oncol*. 2013; 11(1):14–23. Epub 2013/02/19. PubMed Central PMCID: PMC3624708. PMID: [23416859](#)
3. Golabek T, Belsey J, Drewa T, Kolodziej A, Skoneczna I, Milecki P, et al. Evidence-based recommendations on androgen deprivation therapy for localized and advanced prostate cancer. *Cent European J Urol*. 2016; 69(2):131–8. Epub 2016/08/24. PubMed Central PMCID: PMC4986307. doi: [10.5173/cej.2016.812](#) PMID: [27551549](#)
4. Botrel TE, Clark O, Lima Pompeo AC, Horta Bretas FF, Sadi MV, Ferreira U, et al. Efficacy and Safety of Combined Androgen Deprivation Therapy (ADT) and Docetaxel Compared with ADT Alone for Metastatic Hormone-Naive Prostate Cancer: A Systematic Review and Meta-Analysis. *PLoS One*. 2016; 11(6):e0157660. Epub 2016/06/17. PubMed Central PMCID: PMC4911003. doi: [10.1371/journal.pone.0157660](#) PMID: [27308831](#)
5. Ding XF, Huang GM, Shi Y, Li JA, Fang XD. Med19 promotes gastric cancer progression and cellular growth. *Gene*. 2012; 504(2):262–7. Epub 2012/05/09. doi: [10.1016/j.gene.2012.04.033](#) PMID: [22565189](#)
6. Li XH, Fang DN, Zeng CM. Knockdown of MED19 by short hairpin RNA-mediated gene silencing inhibits pancreatic cancer cell proliferation. *Cancer Biother Radiopharm*. 2011; 26(4):495–501. Epub 2011/08/13. doi: [10.1089/cbr.2010.0863](#) PMID: [21834715](#)
7. Liu Y, Tao X, Fan L, Jia L, Gu C, Feng Y. Knockdown of mediator complex subunit 19 inhibits the growth of ovarian cancer. *Mol Med Rep*. 2012; 6(5):1050–6. Epub 2012/09/11. doi: [10.3892/mmr.2012.1065](#) PMID: [22961438](#)

8. Wen H, Feng CC, Ding GX, Meng DL, Ding Q, Fang ZJ, et al. Med19 promotes bone metastasis and invasiveness of bladder urothelial carcinoma via bone morphogenetic protein 2. *Ann Diagn Pathol*. 2013; 17(3):259–64. Epub 2013/01/02. doi: [10.1016/j.anndiagpath.2012.11.004](https://doi.org/10.1016/j.anndiagpath.2012.11.004) PMID: [23276457](https://pubmed.ncbi.nlm.nih.gov/23276457/)
9. Yu S, Xia S, Yang D, Wang K, Yeh S, Gao Z, et al. Androgen receptor in human prostate cancer-associated fibroblasts promotes prostate cancer epithelial cell growth and invasion. *Med Oncol*. 2013; 30(3):674. Epub 2013/08/09. doi: [10.1007/s12032-013-0674-9](https://doi.org/10.1007/s12032-013-0674-9) PMID: [23925662](https://pubmed.ncbi.nlm.nih.gov/23925662/)
10. Conaway RC, Sato S, Tomomori-Sato C, Yao T, Conaway JW. The mammalian Mediator complex and its role in transcriptional regulation. *Trends in biochemical sciences*. 2005; 30(5):250–5. doi: [10.1016/j.tibs.2005.03.002](https://doi.org/10.1016/j.tibs.2005.03.002) PMID: [15896743](https://pubmed.ncbi.nlm.nih.gov/15896743/)
11. Myers LC, Gustafsson CM, Bushnell DA, Lui M, Erdjument-Bromage H, Tempst P, et al. The Med proteins of yeast and their function through the RNA polymerase II carboxy-terminal domain. *Genes & development*. 1998; 12(1):45–54. PubMed Central PMCID: [PMC316402](https://pubmed.ncbi.nlm.nih.gov/PMC316402/).
12. Zhang H, Jiang H, Wang W, Gong J, Zhang L, Chen Z, et al. Expression of Med19 in bladder cancer tissues and its role on bladder cancer cell growth. *Urol Oncol*. 2012; 30(6):920–7. Epub 2011/04/12. doi: [10.1016/j.urolonc.2010.10.003](https://doi.org/10.1016/j.urolonc.2010.10.003) PMID: [21478038](https://pubmed.ncbi.nlm.nih.gov/21478038/)
13. Zhang X, Fan Y, Liu B, Qi X, Guo Z, Li L. Med19 promotes breast cancer cell proliferation by regulating CBFA2T3/HEB expression. *Breast Cancer*. 2016. Epub 2016/08/31.
14. Wei L, Wang XW, Sun JJ, Lv LY, Xie L, Song XR. Knockdown of Med19 suppresses proliferation and enhances chemo-sensitivity to cisplatin in non-small cell lung cancer cells. *Asian Pac J Cancer Prev*. 2015; 16(3):875–80. Epub 2015/03/05. PMID: [25735376](https://pubmed.ncbi.nlm.nih.gov/25735376/)
15. Sun M, Jiang R, Li JD, Luo SL, Gao HW, Jin CY, et al. MED19 promotes proliferation and tumorigenesis of lung cancer. *Mol Cell Biochem*. 2011; 355(1–2):27–33. Epub 2011/04/27. doi: [10.1007/s11010-011-0835-0](https://doi.org/10.1007/s11010-011-0835-0) PMID: [21519921](https://pubmed.ncbi.nlm.nih.gov/21519921/)
16. Xu LL, Guo SL, Ma SR, Luo YA. Mammalian mediator 19 mediates H1299 lung adenocarcinoma cell clone conformation, growth, and metastasis. *Asian Pac J Cancer Prev*. 2012; 13(8):3695–700. Epub 2012/10/27. PMID: [23098456](https://pubmed.ncbi.nlm.nih.gov/23098456/)
17. Wang T, Hao L, Feng Y, Wang G, Qin D, Gu G. Knockdown of MED19 by lentivirus-mediated shRNA in human osteosarcoma cells inhibits cell proliferation by inducing cell cycle arrest in the G0/G1 phase. *Oncol Res*. 2011; 19(5):193–201. Epub 2011/05/06. PMID: [21542455](https://pubmed.ncbi.nlm.nih.gov/21542455/)
18. Zou SW, Ai KX, Wang ZG, Yuan Z, Yan J, Zheng Q. The role of Med19 in the proliferation and tumorigenesis of human hepatocellular carcinoma cells. *Acta Pharmacol Sin*. 2011; 32(3):354–60. Epub 2011/03/05. PubMed Central PMCID: [PMC4002777](https://pubmed.ncbi.nlm.nih.gov/PMC4002777/). doi: [10.1038/aps.2010.223](https://doi.org/10.1038/aps.2010.223) PMID: [21372827](https://pubmed.ncbi.nlm.nih.gov/21372827/)
19. Cui X, Xu D, Lv C, Qu F, He J, Chen M, et al. Suppression of MED19 expression by shRNA induces inhibition of cell proliferation and tumorigenesis in human prostate cancer cells. *BMB Rep*. 2011; 44(8):547–52. Epub 2011/08/30. PMID: [21871180](https://pubmed.ncbi.nlm.nih.gov/21871180/)
20. Imberg-Kazdan K, Ha S, Greenfield A, Poultney CS, Bonneau R, Logan SK, et al. A genome-wide RNA interference screen identifies new regulators of androgen receptor function in prostate cancer cells. *Genome Res*. 2013; 23(4):581–91. Epub 2013/02/14. PubMed Central PMCID: [PMC3613576](https://pubmed.ncbi.nlm.nih.gov/PMC3613576/). doi: [10.1101/gr.144774.112](https://doi.org/10.1101/gr.144774.112) PMID: [23403032](https://pubmed.ncbi.nlm.nih.gov/23403032/)
21. King D, Yeomanson D, Bryant HE. PI3King the lock: targeting the PI3K/Akt/mTOR pathway as a novel therapeutic strategy in neuroblastoma. *J Pediatr Hematol Oncol*. 2015; 37(4):245–51. Epub 2015/03/27. doi: [10.1097/MPH.0000000000000329](https://doi.org/10.1097/MPH.0000000000000329) PMID: [25811750](https://pubmed.ncbi.nlm.nih.gov/25811750/)
22. van Duijn PW, Trapman J. PI3K/Akt signaling regulates p27(kip1) expression via Skp2 in PC3 and DU145 prostate cancer cells, but is not a major factor in p27(kip1) regulation in LNCaP and PC346 cells. *Prostate*. 2006; 66(7):749–60. Epub 2006/01/21. doi: [10.1002/pros.20398](https://doi.org/10.1002/pros.20398) PMID: [16425184](https://pubmed.ncbi.nlm.nih.gov/16425184/)
23. Polyak K, Lee MH, Erdjument-Bromage H, Koff A, Roberts JM, Tempst P, et al. Cloning of p27Kip1, a cyclin-dependent kinase inhibitor and a potential mediator of extracellular antimitogenic signals. *Cell*. 1994; 78(1):59–66. Epub 1994/07/15. PMID: [8033212](https://pubmed.ncbi.nlm.nih.gov/8033212/)
24. Chu IM, Hengst L, Slingerland JM. The Cdk inhibitor p27 in human cancer: prognostic potential and relevance to anticancer therapy. *Nat Rev Cancer*. 2008; 8(4):253–67. Epub 2008/03/21. doi: [10.1038/nrc2347](https://doi.org/10.1038/nrc2347) PMID: [18354415](https://pubmed.ncbi.nlm.nih.gov/18354415/)
25. Singh P, Alex JM, Bast F. Insulin receptor (IR) and insulin-like growth factor receptor 1 (IGF-1R) signaling systems: novel treatment strategies for cancer. *Med Oncol*. 2014; 31(1):805. Epub 2013/12/18. doi: [10.1007/s12032-013-0805-3](https://doi.org/10.1007/s12032-013-0805-3) PMID: [24338270](https://pubmed.ncbi.nlm.nih.gov/24338270/)
26. Broster SA, Kyprianou N. Epithelial-mesenchymal transition in prostatic disease. *Future Oncol*. 2015; 11(23):3197–206. Epub 2015/11/10. doi: [10.2217/fo.15.253](https://doi.org/10.2217/fo.15.253) PMID: [26551285](https://pubmed.ncbi.nlm.nih.gov/26551285/)